

Thermal electron capture by some chlorobromopropanes

W. Barszczewska¹, J. Kopyra¹, J. Wnorowska¹, I. Szamrej^{1,a}, N.L. Asfandiarov²,
S.A. Pshenichnyuk², and S.A. Fal'ko²

¹ Chemistry Department, University of Podlasie, Siedlce, Poland

² Institute of Physics of Molecules and Crystals, Russian Academy of Science, Ufa, Russia

Received 9 March 2005 / Received in final form 12 May 2005

Published online 2nd August 2005 – © EDP Sciences, Società Italiana di Fisica, Springer-Verlag 2005

Abstract. Thermal electron attachment rate constants for $\text{CH}_2\text{ClCHBrCH}_3$ and $\text{CH}_2\text{ClCH}_2\text{CH}_2\text{Br}$ have been measured using electron swarm method. Corresponding rate constants are equal to 3.5×10^{-10} and $2.5 \times 10^{-10} \text{ cm}^3 \text{ molec}^{-1} \text{ s}^{-1}$, respectively. Parallely, negative ion mass spectra of these compounds as well as $\text{CH}_2\text{FCH}_2\text{Br}$, $\text{CH}_2\text{ClCH}_2\text{Br}$, $\text{CH}_2\text{BrCH}_2\text{Br}$ and CF_3CHClBr has been measured with negative ion mass spectrometry method. The rate constants have been compared with the negative ion mass spectra.

PACS. 52.20.-j Elementary processes in plasmas

1 Introduction

This paper deals with thermal electron capture processes by some halocarbons in the gas phase. The data from various laboratories differ quite often by more than an order of magnitude and new data and some theoretical analysis are required to find the correct values [1–4].

The rate constant for the thermal electron capture strongly depends on the extent of overlap between the shape and position of the dissociative electron attachment (DEA) cross-section peak and the Maxwell-Boltzman distribution of both electron and molecules energies [1–3]. The thermal attachment rate constant can be measured in a swarm experiment. The resonance peak can be represented by electron capture negative ion spectra obtained in beam experiment or vertical attachment energy (VAE) obtained from electron transmission spectroscopy (ETS) as in reference [1].

This work is a continuation of our program to measure systematically the rate constants for thermal electron capture by haloalkanes using the electron swarm method. Up to date, the measurements concentrated mostly on halomethanes and haloethanes. In our previous papers we have presented for the first time the rate constants for 1- and 2-chloropropanes and all four isomers of dichloropropane [2] as well as for 1- and 2-bromopropanes [3].

Here we present the swarm rate constants for further two halopropanes 1-chloro,3-bromopropane and 1-chloro,2-bromopropane and their electron capture negative ion mass spectra (ECNI MS) as well as those for 1- and 2-bromopropanes and some bromoethanes: $\text{CH}_2\text{FCH}_2\text{Br}$, $\text{CH}_2\text{ClCH}_2\text{Br}$, $\text{CH}_2\text{BrCH}_2\text{Br}$, CF_3CHClBr .

2 Experimental

The electron capture negative ion mass spectrometry has been used to determine the dependence of the electron attachment process relative cross-section on the electron energy. We could not measure absolute cross-section, so the main result is energy position of the maximum and the shape of the peak.

Negative ion mass spectra have been obtained using a modified MI-1201 mass spectrometer described in detail in previous papers [5–7]. Schematically, the device consists of the anion source (tungsten filament, electron optics and reaction chamber), magnetic analyzer and detection system. In the experiment, an electron beam of the defined energy moved through an equilibrium flow of molecules in the reaction chamber at a pressure ca. 10^{-5} Torr. The negative ions formed were separated according to the mass to charge ratio using 90° magnetic sector analyzer and registered by detection system.

The experimental conditions were as follows: accelerating voltage of the ions 4 kV, electron trap current $\sim 1 \mu\text{A}$ and an electron energy range 0–10 eV. The energy distribution function of the electron beam fwhm was ca. 0.4 eV as determined using the SF_6^- peak from SF_6 . As the energy scale could not be given in absolute units the apparatus was calibrated by putting 0 eV at the maximum of SF_6^- peak (total electron scattering cross-section 10^{-16} cm^2) and 4.4 eV at maximum of the O^- peak from CO_2 (cross-section, $1.7 \times 10^{-19} \text{ cm}^2$) [8,9] (cf. Fig. 1). The calibration did not change appreciably between series of the experiment and was being checked time to time.

The mass spectra were taken at 348–353 K. This (lowest) temperature of the anion source is defined by the temperature of the tungsten filament which is rather close to the ionization chamber.

^a e-mail: iwona@ap.siedlce.pl

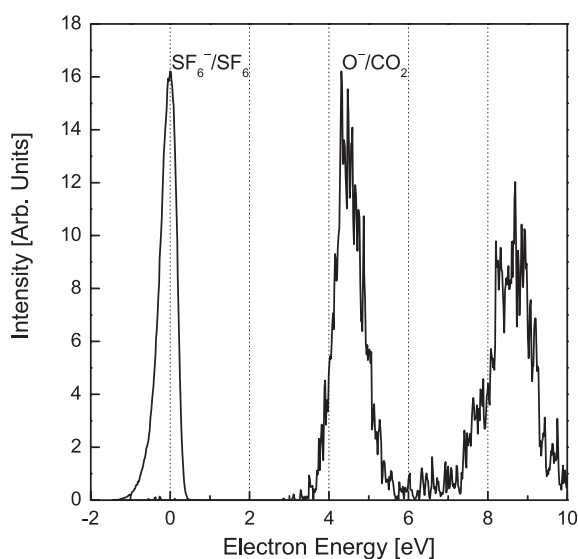


Fig. 1. The NIS spectra for SF_6^- from SF_6 (0 eV) and O^- (4.4 eV) from CO_2 for calibration purpose. The intensity of the SF_6^- is ca. 10 times higher than that of O^- .

An electron swarm method with ionization chamber and carbon dioxide as a carrier gas has been applied for the measurements of the electron capture rate constants. The experimental procedure has been described in detail previously [10]. In brief, an experimental set-up consists of an ionization chamber with two parallel electrodes, a preamplifier, a fast oscilloscope with a digital memory connected with a computer and a computer-controlled power supply.

The electron acceptor was introduced into the ionization chamber in the excess of carbon dioxide as a carrier gas. The electron swarm was produced by an ionization of the carrier gas with an α -particle in the plane parallel to the electrodes. In carbon dioxide electrons are swiftly thermalized [11]. The electron swarm moved to the collecting electrode under the influence of a uniform electric field causing the change in collecting electrode potential which increases linearly as electrons move to the electrode in pure CO_2 . In the presence of an electron acceptor it declines from linearity due to removal of electrons. The preamplifier output potential is registered on the oscilloscope and saved in a computer memory. The analysis of the peak shape gives the rate of the electron capture at given acceptor concentration and hence the corresponding rate constant.

As in all previous experiments (cf. Refs. [2,3] and further Refs. therein) to purify the technical carbon dioxide used in swarm experiment we froze it with liquid nitrogen and pumped out volatile gases. Then the trap was immersed into the dry ice-acetone bath and the gas was introduced to the chamber and the rate of disappearance of electron swarm was measured. It always corresponded to that of a non-attaching gas which also proved that no absorbed electron scavengers were present. Then it was pumped out of the chamber, an electron acceptor was in-

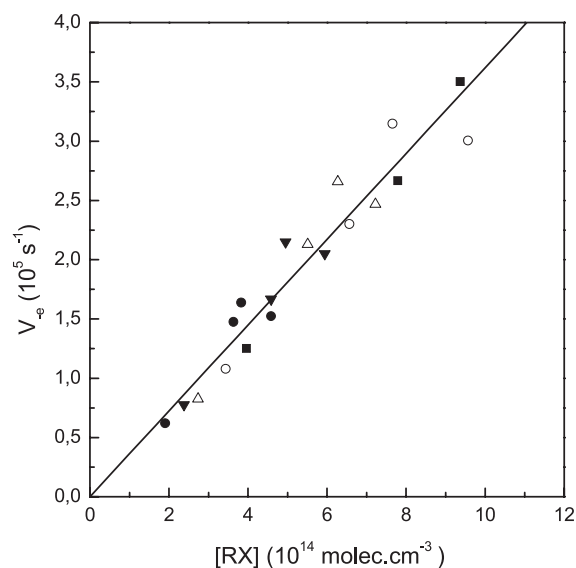


Fig. 2. The rate of electron disappearance from the swarm for $\text{CH}_2\text{ClCHBrCH}_3$ as a function of halocarbon concentration at a few concentrations of carbon dioxide: (■) 2.97, (●) 2.64, (▼) 1.98, (△) 1.65, (○) 1.32×10^{19} molec cm^{-3} .

produced and next portion of CO_2 was introduced to the required overall pressure.

The other gases: 1-chloro-3-bromopropane (Across Organics), 1-chloro,2-bromopropane (Aldrich) were purified by the vacuum freeze-pump-thaw technique. The same samples were used in both beam and swarm experiment.

All the rate constants were measured at room temperature (293 ± 3 K).

The dependence of the electron capture rate on the $\text{CH}_2\text{ClCHBrCH}_3$ concentration at different concentrations of carbon dioxide is shown in Figure 2. One can see that it does not depend on carbon dioxide pressure which again shows that it does not contain impurities influencing the rate constants. Also, we did not observe peaks from impurities in the beam experiment.

The obtained thermal electron capture rate constants are compared with energy positions of the corresponding NIS peaks.

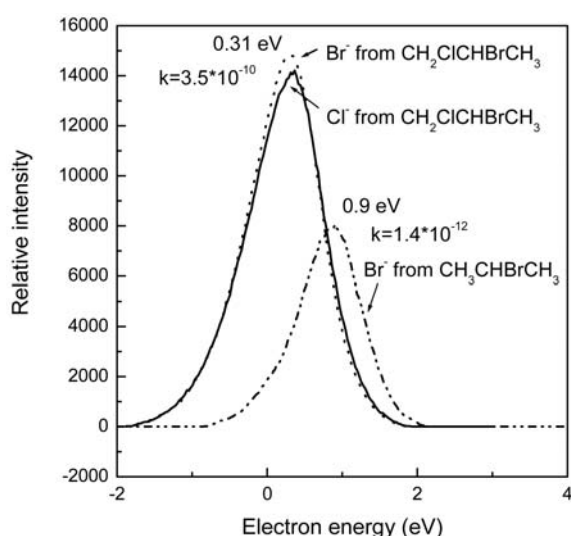
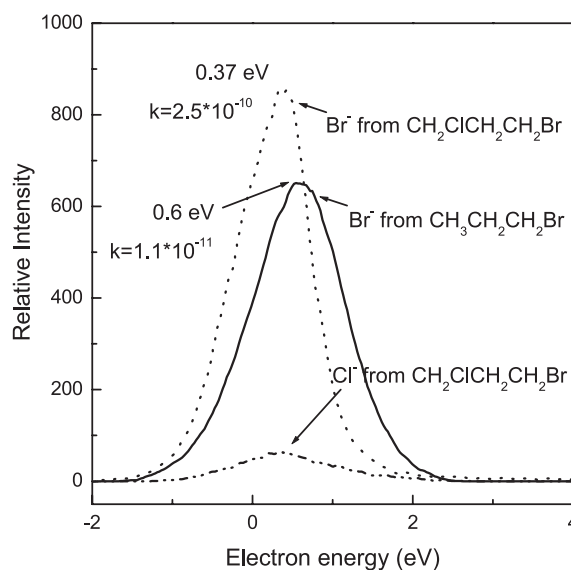
3 Results and discussion

The negative ion mass spectra for $\text{CH}_3\text{CH}_2\text{CH}_2\text{Br}$, $\text{CH}_3\text{CHBrCH}_3$, $\text{CH}_2\text{ClCH}_2\text{CH}_2\text{Br}$, $\text{CH}_2\text{ClCHBrCH}_3$, $\text{CH}_2\text{FCH}_2\text{Br}$, $\text{CH}_2\text{ClCH}_2\text{Br}$, $\text{CH}_2\text{BrCH}_2\text{Br}$ and CF_3CHClBr have been measured.

The values of DEA maximum peak position and the new rate constants are presented in Table 1 together with the previous kinetic data for monobromopropanes and bromoethanes. Figures 3 and 4 show the negative ions spectra (NIS) for $\text{CH}_2\text{ClCHBrCH}_3$ and $\text{CH}_2\text{ClCH}_2\text{CH}_2\text{Br}$. For comparison, also the spectra for $\text{CH}_3\text{CHBrCH}_3$ and $\text{CH}_3\text{CH}_2\text{CH}_2\text{Br}$ are shown. The NIS for haloethanes are quite similar, Br^- being the main anion registered.

Table 1. Measured rate constants for thermal electron capture, k_{th} , and positions of the maxima on negative ion spectra, E_{max} , ([pres] means measured for this paper) together with the literature data where available.

Compound	k_{th} ($\text{cm}^3 \text{molec}^{-1} \text{s}^{-1}$)	E_{max} (eV)
$\text{CH}_3\text{CH}_2\text{Br}$	5.3×10^{-12} [3]	0.6 [13]
$\text{CH}_3\text{CH}_2\text{CH}_2\text{Br}$	1.1×10^{-11} [3]	0.6 [pres], 0.65 [13]
$\text{CH}_3\text{CHBrCH}_3$	1.4×10^{-12} [3]	0.9 [pres], 0.9 [13]
$\text{CH}_2\text{ClCH}_2\text{CH}_2\text{Br}$	$(2.5 \pm 0.2) \times 10^{-10}$ [pres]	0.4 [pres]
$\text{CH}_2\text{ClCHBrCH}_3$	$(3.5 \pm 0.4) \times 10^{-10}$ [pres]	0.3 [pres]
$\text{CH}_2\text{FCH}_2\text{Br}$	5×10^{-11} [3]	0.4 [pres]
$\text{CH}_2\text{ClCH}_2\text{Br}$	4.5×10^{-10} [10]	0.2 [pres]
$\text{CH}_2\text{BrCH}_2\text{Br}$	1.8×10^{-8} [3]	0.15 [pres]
CF_3CHClBr	7×10^{-8} [14]	0.05 [pres]

**Fig. 3.** Negative ions spectra for $\text{CH}_2\text{ClCHBrCH}_3$ and $\text{CH}_3\text{CHBrCH}_3$.**Fig. 4.** Negative ions spectra for $\text{CH}_2\text{ClCH}_2\text{CH}_2\text{Br}$ and $\text{CH}_3\text{CH}_2\text{CH}_2\text{Br}$.

The position of the NIS peak for bromoethanes lowers appreciably when going from 1-bromo- (0.6 eV) through 1-bromo,2-fluoro- (0.4 eV), 1-bromo,2-chloro- (0.2 eV) to 1,2-dibromoethane (0.15 eV). Accordingly, the rate constants increase strongly in this direction: 5.3×10^{-12} , 5×10^{-11} , 4.5×10^{-10} and $1.8 \times 10^{-8} \text{ cm}^3 \text{ molec}^{-1} \text{ s}^{-1}$, respectively. Thus, the second halogen lowers correspondingly the intermediate negative ion energy.

Highly substituted CF_3CHClBr accepts electrons almost at thermal energy and accordingly the rate constant ($k_{th} = 7 \times 10^{-8} \text{ cm}^3 \text{ molec}^{-1} \text{ s}^{-1}$) reaches almost the thermal value ($\approx 10^{-7} \text{ cm}^3 \text{ molec}^{-1} \text{ s}^{-1}$).

For monobromopropanes, changing a position of bromine atom from 2 to 1 causes an increase in the rate constant by one order of magnitude (from 1.4×10^{-12} to $1.1 \times 10^{-11} \text{ cm}^3 \text{ molec}^{-1} \text{ s}^{-1}$) and compatibly lowering the peak position of NIS from 0.9 to 0.6 eV.

An addition of Cl in position 3 in $\text{CH}_2\text{ClCH}_2\text{CH}_2\text{Br}$ (Fig. 4) leads to some lowering the peak position (0.6 and 0.37 eV). At the same time this increases the rate constant

(1.1×10^{-11} to $2.5 \times 10^{-10} \text{ cm}^3 \text{ molec}^{-1} \text{ s}^{-1}$). Also, one observes a minor yield of the Cl^- ion.

An addition of chlorine atom in neighboring position to Br ($\text{CH}_2\text{ClCHBrCH}_3$, Fig. 3) causes a strong increase in the rate constant (from 1.4×10^{-12} to $3.5 \times 10^{-10} \text{ cm}^3 \text{ molec}^{-1} \text{ s}^{-1}$) and correspondingly appreciable decrease in the NIS peak position from 0.9 to 0.31 eV. One can also observe that the intermediate molecular negative ion produces both Br^- and Cl^- ions in almost equal proportions with the same shape of the NIS. This may suggest that both of them are formed from the same intermediate molecular negative ion state.

The ratio of the rate constants for CH_2BrCl [15] and CH_3Br [3,4] (7.1×10^{-9} and $6.6 \times 10^{-12} \text{ cm}^3 \text{ molec}^{-1} \text{ s}^{-1}$, the only data for chlorine and bromine placed at the same carbon atom) is still higher. Thus, one can conclude that the shorter the distance between haloatoms the stronger the influence of the chlorine atom on the electron capture process in bromoalkanes.

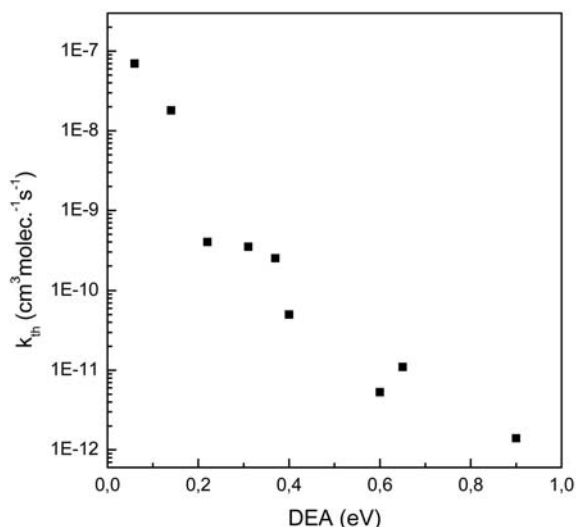


Fig. 5. The k_{th} dependence on DEA position for compounds from Table 1.

The thermal rate constants, DEA cross-sections and VAE are as a rule analyzed separately while they describe the same process and should be interconnected. This follows from the fact that the rate constant for thermal electron capture strongly depends on the extent of overlap between the shape and position of the DEA peak and the Maxwell-Boltzman distribution of both electron and molecules energies. The DEA peak energy position and cross-section, in turn, depend on VAE and partly on autodetachment rate.

In our previous paper [2] we have shown that there is a strong correlation between the thermal electron attachment rate constant and the value of vertical attachment energy measured by Aflatooni et al. [16–18]. Plotting $\log(k_{th})$ vs. VAE we have got good linear dependence for two groups of compounds — chloroalkanes and chlorofluoroalkanes. Also Burrow [1] have shown the same dependence using the k_{th} values calculated from his beam experiment.

For the group of bromoalkanes there are single data on VAE, so for the purpose of further analysis the DEA values have been applied. It is clearly seen from the inspection of the data in Table 1 that the lower the position of the maximum of DEA (E_{max} in Tab. 1) the higher the thermal attachment rate constant. If we plot $\log(k_{th})$ vs. the maximum for DEA peak as is presented in Figure 5 we get a good correlation between these data.

The finding that there is a clear dependence between $\log(k_{th})$ and DEA can be a very good tool not only to predict these values but also, which is even more important, to correct them or to look for some additional, not common, explanation if they do not fit to the picture.

This research was supported in part by NATO grant JSTC.RCLG.979570.

References

1. G.A. Gallup, K. Aflatooni, P.D. Burrow, *J. Chem. Phys.* **118**, 2562 (2003)
2. W. Barszczewska, J. Kopyra, J. Wnorowska, I. Szamrej, *J. Phys. Chem. A* **107**, 11427 (2003)
3. W. Barszczewska, J. Kopyra, J. Wnorowska, I. Szamrej, *Int. J. Mass Spectrom.* **233**, 199 (2004)
4. L.G. Christophorou, *Z. Phys. Chem.* **195**, 195 (1996)
5. S.A. Pshenichnyuk, N.L. Asfandiarov, V.S. Fal'ko, V.G. Lukin, *Int. J. Mass Spectrom.* **227**, 259 (2003)
6. N.L. Asfandiarov, S.A. Pshenichnyuk, V.S. Fal'ko, J. Wnorowska, K. Wnorowski, I. Szamrej, *Nukleonika* **48**, 83 (2003)
7. N.L. Asfandiarov, S.A. Pshenichnyuk, A.I. Fokin, E.P. Nafikova, *Chem. Phys.* **298**, 263 (2004)
8. A. Stamatovič, G.J. Schulz, *Phys. Rev. A* **7**, 589 (1973)
9. L.G. Christophorou, *Electron-Molecule Interactions and their Applications* (Academic Press, Orlando, 1984), Vol. 1
10. A. Rosa, W. Barszczewska, M. Foryś, I. Szamrej, *Int. J. Mass Spectrom.* **205**, 85 (2001)
11. I. Szamrej, M. Foryś, *Rad. Phys. Chem.* **33**, 393 (1989)
12. I. Szamrej, M. Foryś, N.L. Asfandiarov, in *Gaseous Dielectrics X*, edited by L.G. Christophorou et al. (Springer, New York, 2004)
13. A. Modelli, D. Jones, *J. Phys. Chem.* **108**, 417 (2004)
14. W. Barszczewska, J. Kopyra, J. Wnorowska, I. Szamrej, M. Foryś, in *Gaseous Dielectrics IX*, edited by L.G. Christophorou et al. (Kluwer Academic/Plenum Publishers, New York, 2001)
15. T. Sunagawa, H. Shimamori, *J. Chem. Phys.* **107**, 7876 (1997)
16. K. Aflatooni, P.D. Burrow, *Int. J. Mass Spectrom.* **205**, 149 (2001)
17. K. Aflatooni, P.D. Burrow, *J. Chem. Phys.* **113**, 1455 (2000)
18. K. Aflatooni, G.A. Gallup, P.D. Burrow, *Chem. Phys. Lett.* **282**, 398 (1998)